ELSEVIER

Catalysis Today 54 (1999) 165–180

CATALYSIS TODAY

www.elsevier.com/locate/cattod

Catalytic combustion for the production of energy

Pio Forzatti *, Gianpiero Groppi

Dipartimento di Chimica Industriale e Ingegneria Chimica 'G. Natta' del Politecnico, Pza Leonardo da Vinci 32, 20133 Milan, Italy

Abstract

In this paper, attention is focused on adiabatic lean-premixed catalytic combustion, which has attracted interest in the last decades as an environmentally friendly and cost-effective alternative to flame combustion for power generation by gas turbines.

The different configurations of the combustion systems for gas turbines are presented. and the results of pilot tests, full-scale bench tests and field trials with retrofitted machines are illustrated. The relevant physico-chemical and catalytic properties of highly active supported PdO catalysts, including reversible PdO–Pd transformation and low-temperature activity, are then addressed. The structural and catalytic properties of highly stable metal substituted hexaaluminates are also discussed. The use of fuel alternative to natural gas is briefly covered. The relevant features of mathematical models for both, the catalyst section and the homogeneous section, that can be used in the design and analysis of the catalytic combustor, are described and the major conclusions of the modelling activity are outlined. Finally, the research opportunities in the area are discussed.

Keywords: Gas turbine combustors; NO_x reduction; Methane combustion; Palladium catalyst; Hexaaluminates; Mathematical Modelling

1. Introduction

In the last decades, catalytic combustion has been vigorously explored as a route to the production of heat and energy in view of its capability to achieve effective combustion at much lower temperatures than in conventional flame combustion, thus allowing for the simultaneous ultra-low emissions of NO_x, CO and Unburned Hydrocarbons (UHC) [1–12].

Various concepts of catalytic combustion have been investigated. and these can be classified into the following three groups:

1. adiabatic lean-premixed catalytic combustion, which has attracted attention for power generation by gas turbines (GT) [8];
2. non-adiabatic premixed catalytic combustion, which is under development for several applications including premixed fibre burners, domestic boilers and compact chemical reactor heaters [13–17]; and
3. non-adiabatic diffusive catalytic combustion, that has been commercially applied in radiant heaters [1].

In this paper, attention is focused on the first concept. Adiabatic lean-premixed catalytic combustion is an environmentally-driven technology that has the potential to achieve NO_x-emissions below 3–5 ppm from natural gas-fired turbines, without incurring additional capital and operating costs associated with the current technology based on steam injection or lean-premixed homogeneous combustion and SCR systems. The development of the technology has required an integrated approach based on the design of advanced combustor configurations and on the development of catalytic

* Corresponding author. Tel.: +39-02-23993238; fax: +39-02-70638173
E-mail address: pio.forzatti@polimi.it (P. Forzatti)

0920-5861/99/$ – see front matter
PII: S0920-5861(99)00178-9

materials with superior activity and stability and unique temperature self-regulating properties.

First, the different designs of the combustion systems for gas turbines are presented and the results of pilot tests, full-scale bench tests and field trials with retrofitted machines are illustrated. The relevant physico-chemical and catalytic properties of highly active supported PdO and highly stable metal-substituted hexaaluminates are then addressed. The use of fuels alternative to natural gas, including low-heating value (LHV) mixtures from biomasses gasification and diesel fuels, are discussed. The use of mathematical models as a tool in the design and analysis of the catalytic combustion system is also covered. The relevant features of mathematical models for both, the catalyst section and the homogeneous section are described and the major conclusions of the modelling activity are outlined. Finally, the research opportunities in the area are briefly illustrated.

2. Configurations and performances of the catalytic combustion systems

The buildup of a gas turbine with a conventional flame combustion system and with a catalytic combustion system are illustrated in Fig. 1 [18]. In a conventional flame combustion system, air enters the combustor at the compressor discharge temperature and, upon blending with fuel, the mixture is ignited and burned at temperatures up to 1800°C. Since the turbine materials cannot withstand this temperature, part of the compressed air is bypassed to the gas, exiting the combustion chamber to reduce the temperature for delivery to the turbine inlet. In the catalytic combustion system, the combustion is accomplished at lower temperature, up to 1100–1300°C. Still, the design criteria and the operating conditions of a catalytic combustor are very severe (see Table 1): ultra low single-digit emissions for NO_x, CO and UHC and catalyst durability exceeding 8 h must be ensured operating at very high gas velocities (in the range of 10–40 m/s referred to the cross section immediately upstream of the catalyst section), with a small overall pressure drop and at very short residence times. This poses the following requirements:

1. very high catalytic activity in methane complete oxidation to ensure ignition at temperatures as close as possible to that of compressed air, in order to minimise the temperature rise provided by the pre-burner that is responsible for most of NO_x formation;
2. high thermal stability of the catalytic materials with respect to deactivation by sintering, phase transformation and volatilisation, and structural integrity upon thermal shocks;

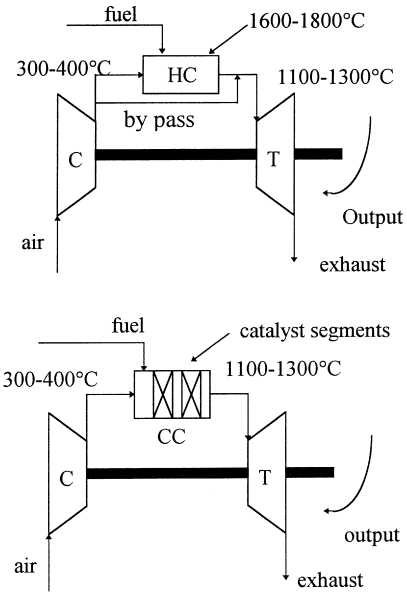

Fig. 1. Schematic of conventional flame and catalytic combustion systems [18]. C, Compressor; T, turbine; HC, homogeneous combustor; CC, catalytic combustor.

Table 1
Design criteria and operating conditions of gas turbine combustors

Design criteria	
Emission targets	$NO_x < 5$ ppm CO < 10 ppm UHC < 10 ppm
Pressure drops	<5%
Catalyst durability	8000 h
Operating conditions	
Inlet temperature	300–450°C
Outlet temperature	1100–1300°C
Pressure	10–20 atm.
Mass flow rate	100–200 kg/m^2 s
Residence time	10–30 ms

	Kind of Catalyst	Cell Number	Height
A	Palladium-cordierite	200 cpi	3 x 20 mm
B			
C			
D	Mn-substituted hexaaluminate sintered at 1200°C	300 cpi	2 x 20 mm
E			
F	Mn-substituted hexaaluminate sintered at 1300°C	300 cpi	2 X 20 mm
G			

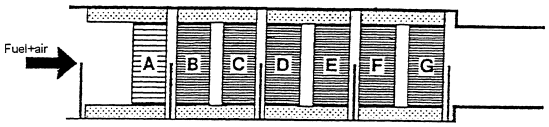

Fig. 2. CST combustor configuration [19].

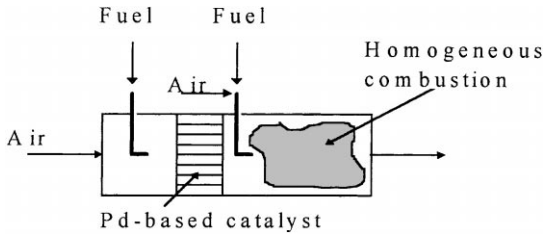

Fig. 3. Schematic of hybrid combustor configuration [21].

3. coupling of the heterogeneous and homogeneous reactions to guarantee complete conversion of the hydrocarbon and ultra low emissions of CO.

Figs. 2–4 show the three alternative approaches that have attracted most attention.

In the first configuration (Fig. 2), the premixed air/fuel stream is fed to multiple catalyst system where the combustion proceeds until complete fuel consumption [12,19]. Typically, one or more monolith honeycomb segments made of Pd on cordierite coated with stabilised alumina are positioned at the entrance to ignite the methane combustion reaction, whereas several less active Mn-substituted hexaaluminate monolith segments sintered at higher temperatures (e.g. 1200°C and 1300°C) are used downstream. These latter materials, first developed by Arai et al. [20], were selected in view of their combustion activity, excellent high-T thermal stability and capability of forming active monolithic honeycombs. The applicability of this system has been demonstrated by Osaka Gas through tests on a 160-kW prototype device, which was operated under representative conditions of a 1.5-MW gas turbine [12,19]. However. the throughput of this system is so low that installing it on a conventional compact engine package may not be possible. In view of this, its commercialisation has been suspended [12]. Furthermore. this system can hardly be upgraded in view of the expected developments of the GT technology towards higher turbine inlet temperature.

In the second configuration (Fig. 3), only a fraction of the fuel is fed to the catalyst; here, the inlet fuel-to-air ratio is carefully adjusted to limit the adiabatic reaction temperature, typically below 1000°C; thus reducing the thermal stresses and preventing catalyst deterioration [21]. The remaining amount of fuel, upon premixing with most of residual air (typically 65% of the overall air flow rate is split for the catalyst, 30% for the premixing nozzles and 5% for cooling and leaking), is fed to a downstream homogeneous section, where combustion is assisted and stabilised by the hot gas exiting the catalyst. In addition to reduction of catalyst thermal stresses and stabilisation of homogeneous premixed combustion at lower temperatures, the following major advantages have been claimed:

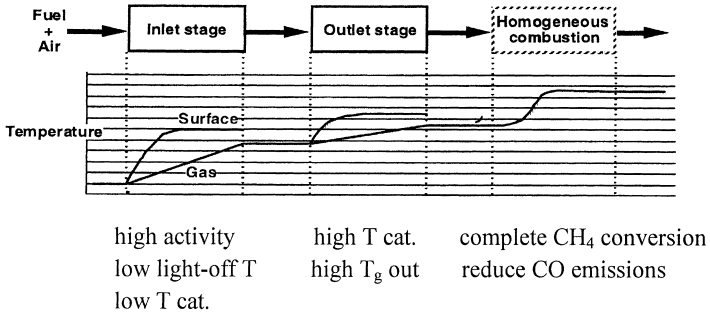

Fig. 4. Partial combustor configuration: XONON technology [26].

Table 2
Tested performances of hybrid combustor [21]

Full scale tests at base load conditions of a 10 MW GT
$NO_x < 5$ ppm (at 16% O_2)
CO + UHC < 9 ppm
Pressure drop < 4%

1. stable combustion is realised under a wider range of combustor operating conditions by controlling the fuel split to the catalyst;
2. a certain degree of lack of uniformity in the fuel/air mixture to the catalytic section is allowed due to the low catalyst temperature.

This configuration was tested by CRIEPI and Kansai Electric in Japan at a scale equivalent to one combustor of a 10-MW class, multi-can type GT [21]. At base load conditions, the design targets on emissions ($NO_x < 5$ ppm, CO and UHC < 10 ppm) and pressure drops (<5%) have been demonstrated for combustor outlet gas temperature of 1350°C (see Table 2). The key factors in such achievements were reported as follows:

1. development of a highly active catalyst made of PdO, promoted with small amounts of Pt and Rh, and supported on an Al_2O_3/ZrO_2 washcoat deposited on honeycomb type monolith made of cordierite;
2. arrangement of the catalyst section and the fuel distribution system in a configuration suitable to optimise the interaction between the heterogeneous and the homogeneous sections within acceptable pressure drops.

Nevertheless, the long-term performance of the catalyst and of the combustor has to be estimated and the control method established.

The third configuration has been developed by Catalytica in co-operation with Tanaka Kikinzoku Kogyo KK and GT manufacturers (e.g. General Electric, Solar Turbines, Allison Engine) [22–24]. In this configuration (see Fig. 4) ,all the fuel, except that required for the pre-burner, is fed to the catalyst section consisting of an inlet stage designed to provide high catalytic activity, low light-off temperature and low catalyst wall temperature and an outer stage designed to operate at higher wall temperatures in order to provide the required high outlet gas temperature. In a downstream homogeneous section, the combustion of the fuel is completed, CO and hydrocarbons are burned out to the levels required to meet the emission standards and the combustor outlet temperature is raised to the levels of modern high efficiency GT, i.e. 1250–1450°C. The control of the maximum catalyst wall temperature is achieved by means of a proprietary catalyst design based on the temperature self-moderating properties of PdO/Pd catalysts in methane combustion, the use of a monolithic metal support with integral heat-exchange capabilities between active and passive channels, and the use of a diffusion barrier over the catalyst surface. These features will be discussed in a following paragraph.

During bench tests at full scale, performed in a catalytic combustor system developed by GE for its MS9001E gas turbine, NO_x, CO, and UHC emissions were documented at levels below the emission targets of 5, 10, and 10 ppm, respectively, at both base load (100%) and part load (78%) (see Table 3) [25]. The tests also documented negligible pressure dynamics. Besides, in a field test performed on a 1.5-MW Kawasaki M1A-13A machine, the system demonstrated stable performance with a negligible loss of

Table 3
Tested performances of XONON combustor

Full scale tests at GE 9E GT conditions [25]
Emissions (15% O_2)
NO_x 3.3 ppm
CO 2.0 ppm
UHC < 0.1 ppm
Pressure drop 2.6%
Combustor dynamics
good mechanical stability and low pressure dynamics
Field tests on 1.5 MW Kawasaki GT [10]
Emissions (15% O_2)
NO_x < 3 ppm
CO < 5 ppm
UHC < 5 ppm
Efficiency 23.0% (23.6%[a])
Load range 50–100%
Durability > 1000 h

[a] Efficiency before introduction of the catalyst.

efficiency and with ultra-low emissions of NO_x, CO and UHC during the 1000-h operation [10].

As shown in Fig. 5, stable operation with low emissions are achieved within an operation window that is bounded by the following conditions [25,26]:

1. the inlet gas temperature must be high enough to ignite the catalyst;
2. the gas temperature at the catalyst exit must be high enough to stabilise homogeneous combustion and the adiabatic combustion temperature must be high enough to ensure complete burnout of HC and CO within the available contact time;
3. the maximum catalyst wall temperature must be low enough to ensure long-term catalyst durability.

Notice that all portion of the catalytic reactor must be within the operating window; accordingly, a good uniformity of inlet fuel-to-air ratio (e.g. ±5%) and of inlet catalyst temperature (e.g. $\Delta T = 18^{\circ}C$) has to be ensured. Catalytica has recently announced the commercialisation of this technology.

3. Combustion catalysts

The catalysts that have been most extensively investigated for GT applications are Pd-supported materials and metal-substituted hexaaluminates.

3.1. Palladium-based catalysts

Palladium oxide supported on alumina or zirconia with various additives is the catalyst of choice for the combustion of methane primarily in view of the following properties:

1. superior activity in the combustion reaction, which results in low light-off temperatures;
2. unique capability of temperature self-control associated with the PdO–Pd reversible transformation;
3. low volatility of Pd species that may be present under reaction conditions (metal, oxides, hydroxides and oxyhydroxides).

The characteristics of the PdO–Pd transformation, its relevance to methane combustion and the low-temperature activity of PdO catalysts are addressed below.

3.1.1. Characteristics of the PdO–Pd transformation

The PdO–Pd transformation has been investigated in the literature primarily by means of TG analysis [27]. Fig. 6 shows the TGA profiles collected by heating and cooling a PdO-on-alumina catalyst, previously calcined at 1000°C for 10 h. Above 800°C, PdO decomposition to Pd metal occurs and is complete at around 900°C. The observed weight loss corresponds well to the calculated value for the amount of PdO present. During the cooling ramp re-oxidation of palladium metal occurs at about 680°C and is complete at 550°C. However, the weight increase is lower than that observed during the decomposition. Different extents of re-oxidation of Pd metal have been reported in the literature, ranging from 30 to 80% by weight [26,27]. Such variations possibly depend on different catalyst pre-treatment. The temperature difference between decomposition and re-oxidation represents a hysteresis of about 150°C. In the second, and the following cycles, PdO decomposes in two distinct steps at 800–850°C and 850–900°C and re-oxidises below 650°C and its magnitude is comparable to those of the first cycle. A third cycle provides essentially the same results as the second one. It has been demonstrated that re-oxidation is not simply a time–temperature rate process, but requires a specific temperature. Indeed no re-oxidation was observed when the sample, after decomposition, was hold for 30 min slightly above the

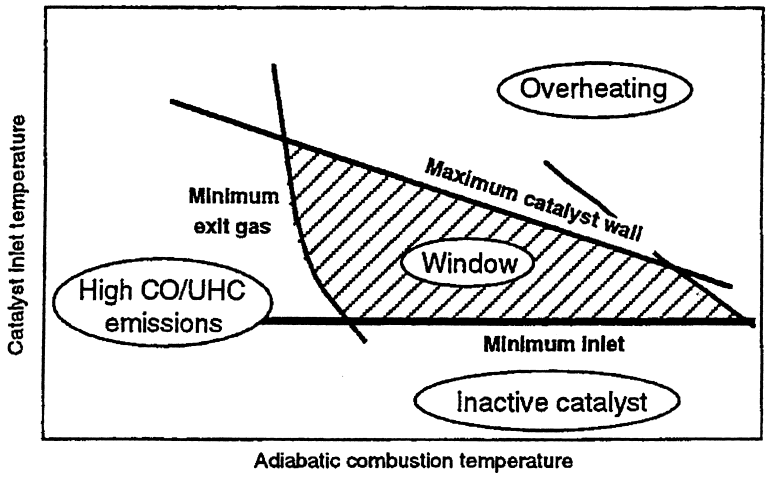

Fig. 5. Operation window in XONON technology [27].

temperature at which the onset of PdO reformation was observed upon cooling [27]. On the other hand, re-oxidation did occur at higher temperatures if only the first reduction step has proceeded. In repeated experiments, where the temperature ramp in the second cycle was reversed after the first weight loss, a distinct weight gain was observed even at 740°C [28]. Using high-temperature X-ray diffraction PdO is the only detectable palladium phase prior to decomposition. Pd metal and PdO are both observed in the course of decomposition and only Pd metal is present when decomposition is complete. Following re-oxidation, both PdO and Pd metal were detected, in line with incomplete PdO reformation during cooling shown by TGA data. The X-ray calculated crystal dimensions of PdO were found to be significantly smaller than those of Pd metal, indicating that palladium sinters upon decomposition to the metal and re-disperses with reformation of the oxide. The tendency of metal palladium particles to sinter easily and to re-disperse during oxidation is well documented in the literature [29–35]. In addition to bulk PdO, evidences for other forms of Pd oxides and for strong palladium-support interactions have also been reported in the literature [36–40].

Table 4 shows that the temperatures of onset of the decomposition of PdO to palladium metal during heating (TD), the temperatures of onset of the re-oxidation of Pd metal during cooling (TR), and the extent of hysteresis (TD–TR), for unsupported PdO and for PdO supported on several oxides. It appears that the temperature of decomposition of the oxide (TD) is only marginally affected by the support, whereas the temperature of re-formation of the oxide from the metal (TR) is markedly affected by the nature of the support;

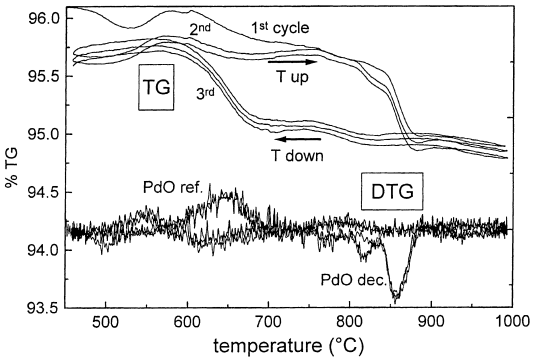

Fig. 6. TG and DTG profiles of Pd/Al_2O_3 during heating and cooling cycles.

Table 4
Temperatures of onset of PdO decomposition (TD1>: 1st stage; TD2 2nd stage) and reformation (TR) on different supports

Support	TD1(°C)	TD2(°C)	TR(°C)	TD1-TR
Unsupported PdO	810	n.o.	785	25
Al_2O_3	795	840	690	105
La_2O_3/Al_2O_3	800	835	690	110
CeO_2/Al_2O_3	800	845	755	45
$CeO_2/La_2O_3/Al_2O_3$	800	840	750	50
ZrO_2	800	860	730	70

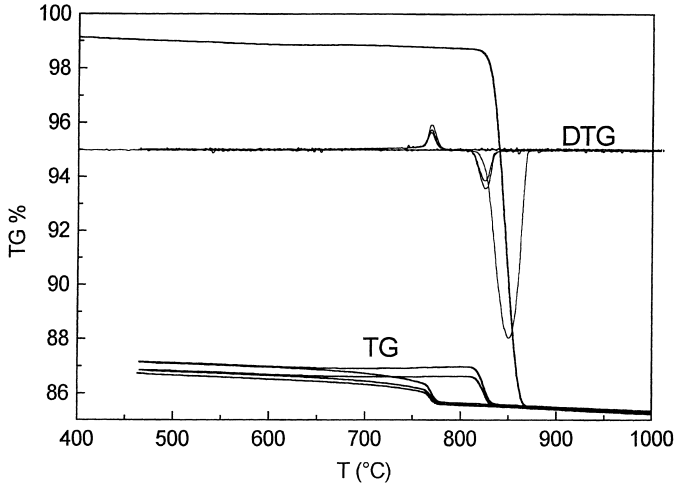

Fig. 7. TG and DTG profiles of bulk PdO during heating and cooling cycles.

accordingly, the extent of hysteresis (TD–TR) is also strongly influenced by the support.

Fig. 7 has been generated according to data collected in our laboratory in similar TG cycles using unsupported PdO powder. During the first heating ramp, PdO decomposes to Pd metal with only one sharp weight loss between 810°C and 870°C. In the cooling curve, only a small weight gain is observed at about 780°C with a magnitude of about 10% of the initial weight loss. In the second cycle, only one weight loss is observed between 810 and 840°C corresponding to reduction of the reformed PdO_x. These results closely resemble those previously obtained by Farrauto et al. [27], but for the magnitude of the weight gain in the first cooling stage that amounted to about 1% of the initial weight loss. However, the characteristic of PdO/Pd transformation in bulk palladium oxide markedly deviates from those observed in supported catalysts, indicating a key role of the support that deserves further investigation.

The temperature of onset of PdO decomposition as a function of the oxygen partial pressure is plotted in Fig. 8 for both, unsupported and supported PdO. A good agreement is observed between experimental data and predictions provided by the relationship that can be derived, assuming that the process is governed by the thermodynamics of the decomposition of bulk PdO, namely $PdO \rightarrow Pd + (1/2)O_2$. This implies that TD in air shifts from 790°C at atmospheric pressure to 980°C at 16 atm. The kinetics of the decomposition process and the related mechanism have been studied so far under conditions far from those of interest for GT applications, e.g. at low temperatures and under vacuum or reducing atmospheres containing H_2 or CH_4 [36,41,42]. Accordingly, these points deserve further investigation.

The mechanism of Pd metal particle re-oxidation at low temperatures is believed to occur through oxygen chemisorption to form a PdO_x surface layer followed by bulk oxidation of the metallic core characterised by a high activation energy of about 100 kJ/mol [27,29–32,36,37,41,42]. The kinetics of the re-oxidation process has been ascribed either to electric field-driven transport of oxygen anions till the oxide layer is sufficiently thick and, thereafter, to the diffusion of oxygen through the oxide layer or to lattice rearrangement needed for the formation of the oxide layer at the oxide-metal interface.

On the other hand, the Pd metal re-oxidation during the cooling cycles at high temperatures, that is of interest for GT applications, is a complex and poorly understood process. The hysteresis between PdO decomposition and Pd metal re-oxidation has been tentatively associated with the capability of Pd metal to chemisorb O_2 only below TD [27] or to the formation of a passive layer of chemisorbed oxygen [43]. However, the first explanation can hardly account for the large difference in the extent of hysteresis observed for

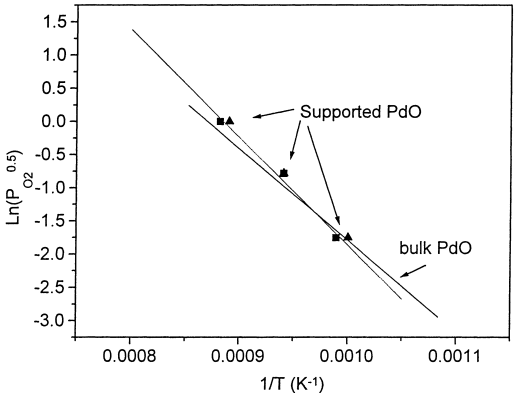

Fig. 8. Thermodynamic control of the first PdO decomposition step: ln (P_{O_2}) vs. 1/TD1. Data for bulk PdO derived from Ref. [83].

unsupported PdO (TD–TR = 25–40°C) and supported PdO (e.g. TD–TR = 120°C for PdO on alumina) and its dependence on the nature of the support. The second explanation as well has not been corroborated by direct evidence for the presence of the passive oxide layer; besides, it is not clear why the passive oxide layer should not be effective below the threshold temperature of Pd metal re-oxidation.

3.1.2. Relevance of PdO–Pd transformation in methane combustion

The methane conversion measured during a catalytic test accomplished by ramping the furnace to a maximum temperature of 900°C, holding for a limited time and then cooling the reactor is shown in Fig. 9. During heating, methane conversion increases with temperature, and is complete above 500°C up to 900°C, well beyond the decomposition temperature of PdO to Pd metal (solid line). When the temperature ramp is reversed and the catalyst is cooled in CH_4/air at about 780°C, the conversion reduces and follows the pattern observed in the presence of the alumina support only (not reported in the figure), thus demonstrating that the catalyst has lost its activity upon complete reduction of PdO to Pd metal. On further cooling, there is a sudden restoration of activity, beginning slightly before re-oxidation of Pd metal to PdO is observed in TG experiments with similar oxygen partial pressure. There is a general consensus in the literature that while PdO is highly active in methane combustion, when only Pd metal is present at high temperatures, the catalyst is inactive. However, there are also indications that the partial reduction of PdO results in a significant enhancement of the methane combustion activity; this was ascribed to the role of Pd metal in the activation of methane through dissociative adsorption [44,45]. Lyubowski and Pfefferle [46], along similar lines, associated the anomalous increase of CH_4 combustion activity observed during cooling ramp in CH_4 air mixtures with the formation of a small cluster of Pd oxide dispersed onto the surface of large Pd metal crystallites. Recently, Fujimoto et al. [47] have hypothesised that activation of methane does not involve Pd metal, but occurs on site pairs consisting of oxygen atoms and oxygen vacancies on the surface of palladium oxide crystallites.

The variations of activity associated with the PdO–Pd reversible thermal transformation are responsible for the unique self-regulating capability of Pd catalysts in methane combustion under adiabatic conditions. However, runaway ignition during start-up has been reported in the literature [48,49], which indicates that the dynamics of the combustion reaction does compete with the dynamics of PdO–Pd transformation. The dynamics of this transformation has not been studied so far at the temperature of interest for GT applications and deserve further investigation. In order to control (or to mitigate) runaway combustion in the case of methane-to-air ratio corresponding to high adiabatic temperatures, the use of zirconia as a support is claimed in the patent literature [49].

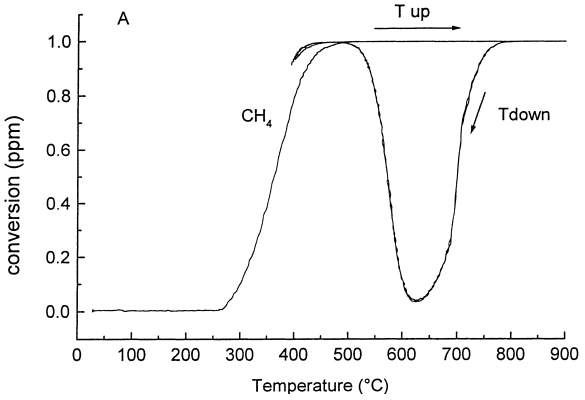

Fig. 9. CH_4 combustion activity during heating and cooling ramps over PdO supported on La_2O_3 stabilised alumina.

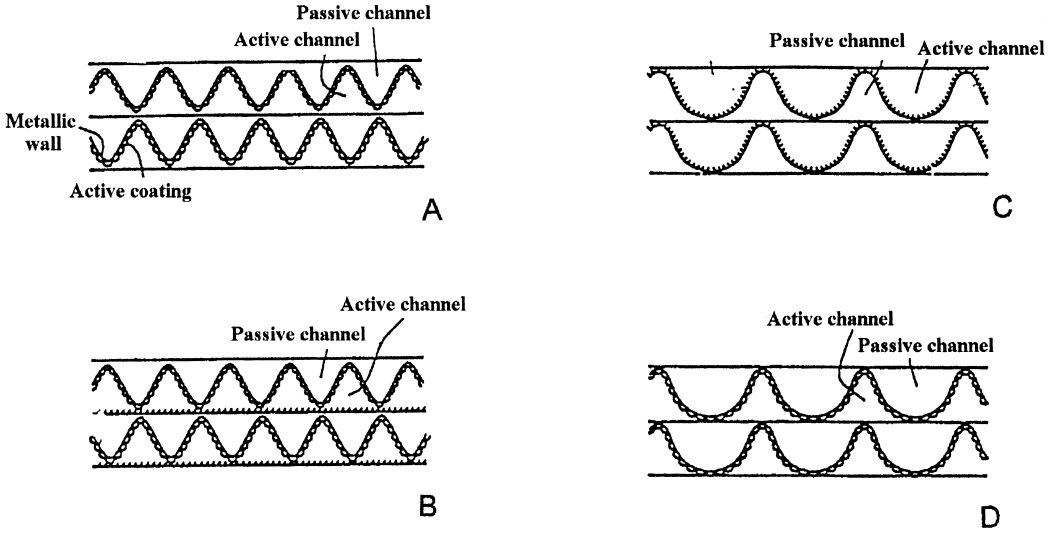

Fig. 10. Examples of coupling of active and passive channels [23].

Table 5
Turnover rates (TOR) of CH_4 combustion over palladium catalysts

TOR (s^{-1})[a]	Crystal size (nm)	Reference
7×10^{-3}–1×10^{-1}	1.4–5.6	[50]
1×10^{-4}–2×10^{-2}	1–30	[34]
3×10^{-3}	3	[51]
3×10^{-2}	16	[52]
1×10^{-4}–2×10^{-2}	2–80	[53]
2×10^{-2}–8×10^{-2}	2–110	[54]
3×10^{-2}–1.8×10^{-1}	3–10	[47]
1×10^{-2}–1×10^{-1}	10–15	Our laboratory

[a] At 550 K and 2% of CH_4.

A diffusion barrier added on the top of the catalyst layer to limit the supply of fuel and/or oxidant to the catalyst, which decreases the apparent activation energy of the combustion reaction, is also recommended [49]. Besides, metal monoliths are preferred and the catalyst is applied to only one side of the monolith structure, as depicted in Fig. 10. In this way, the heat generated inside the active channel is transferred to the nearby inactive channel by conduction through the washcoat and the metal [23,24].

3.1.3. Low-temperature activity of Pd catalysts

The low-temperature activity represents an important issue of PdO catalysts, since it affects the light-off performances of the system. As shown in Table 5, the activity data of methane combustion over PdO based catalysts are widely scattered. Indeed, the conversion levels depend on several critical factors that, in many cases, have not been taken into consideration: e.g. the catalyst pre-treatment procedures, the nature of the Pd precursor, the presence of water in the reaction mixture, and several features of the PdO–Pd transformation. Ribeiro et al. [54] noticed that, provided that these factors are properly accounted for, the turnover rate (TOR) of the reaction is only marginally affected when the support, Pd precursor, and Pd particle sizes are changed. On the other hand, for PdO/ZrO_2, a slight increase of TOR with PdO crystal size in the 3–10 nm range has been recently reported [47].

A relevant feature of commercial Pd catalysts for GT application is represented by the high Pd loading, that is usually in the 10–15% w/w range. Table 6 shows the temperatures where 20% conversion has

Table 6
Effect of Pd loading on an La_2O_3/Al_2O_3 support on PdO crystal size and CH_4 combustion activity[a]

Pd load (w/w)	$T_{20\%}$ (°C)	τ_{PdO}(nm)
2.5	350	12
5	340	10
10	320	13
15	300	13
20	300	12

[a] Test conditions: GHSV = 210,000 Ncc/gh; $Y_{CH_4} = 0.005$.

been measured over Pd supported on stabilised alumina catalysts prepared in our laboratory, together with dimension of the PdO crystallites calculated by XRD. The activity of the catalysts increases markedly with the PdO loading up to 15% w/w and then tends to level off. Accordingly, high Pd loading is required to ensure low light-off temperatures. On the other hand, the size of PdO particles is not affected by the PdO loading: the dimensions of the PdO crystallites compare well with those of the catalyst pores, which indicates that sintering of PdO is controlled by the morphology of the washcoat.

The assessment of a reliable kinetics for the combustion of methane over PdO catalysts is another important issue for the development of catalytic combustors. Kinetic studies in the literature have been customarily performed under conditions far from those of real interest, namely at low GHSV, low temperatures, atmospheric pressure, and using a micro-flow reactor operated with diluted gas feed at low conversions. Under such conditions, the methane combustion was found to be of the first order with respect to methane and zero order with respect to oxygen. Inhibition by CO_2 at concentrations above 0.5% by volume has been measured by Ribeiro et al. [54], but it was not confirmed by other authors [34,55]. On the other hand, strong inhibition by water has been observed, that is expectedly less important at high temperatures. Apparent activation energies of 70–90 and ∼150 kJ/mol have been calculated in the absence, and in the presence, of water in the feed respectively. Such values can be reconciled if water inhibition is accounted for in the analysis [55].

As the kinetic studies are customarily performed under conditions far from reality, extrapolation of the kinetics to actual operating ranges may be critical and must be properly checked. This has been attempted for, instance, by performing ignition/extinction tests. In these tests, the reaction was accomplished at 11 atm and with a flow rate of 9300 SLPM. The feed gas was heated and cooled while the fuel-to-air ratio was varied in order to keep constant the adiabatic reaction temperature [56]. Typical ignition/extinction curves are shown in Fig. 11: the large hysteresis between ignition and extinction temperatures is typical of strongly exothermic reactions. By comparing the results obtained providing a 200°C temperature rise either with only electrical preheating of the feed or

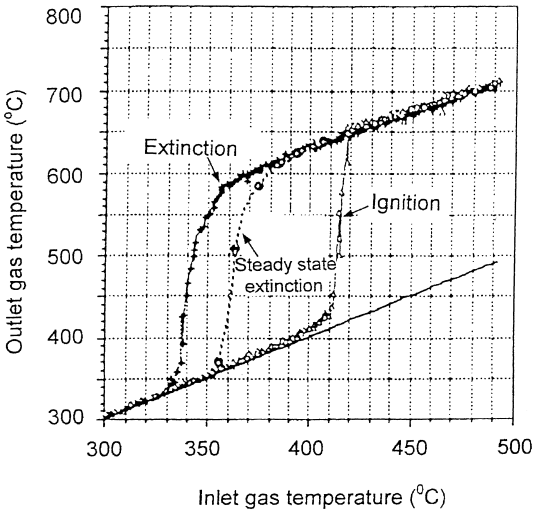

Fig. 11. Ignition/extinction curves in pilot scale combustors [8].

with a pre-burner, it has been demonstrated that the effect of water and CO_2 produced by the pre-burner is small. The temperature shifts to higher values of 18°C for ignition and 12°C for extinction were taken as an indication that water inhibition is significantly reduced under real operation.

In order to develop representative kinetics. however, it is important to collect laboratory-scale kinetic data under conditions as close as possible to the industrial ones. In this respect, a promising device is the annular reactor proposed by McCarty [43]. It consists of two coaxial tubes: the inner ceramic one, is externally coated with the catalyst; the outer one is made of quartz. Such a configuration allows for operation at extremely high space velocities and negligible pressure drops; it also favours heat dispersion through radiation and can provide data under controlled conditions, e.g. with respect to transport limitations. Accordingly, data can be collected in the temperature range close to those of interest for industrial applications. A characterisation of this reactor from the engineering point of view is given in [57].

3.2. Metal substituted hexaaluminate catalysts

Hexaaluminate materials first developed by Arai et al. [20,58] have been extensively investigated for GT applications in view of excellent thermal stability and catalytic activity [59].

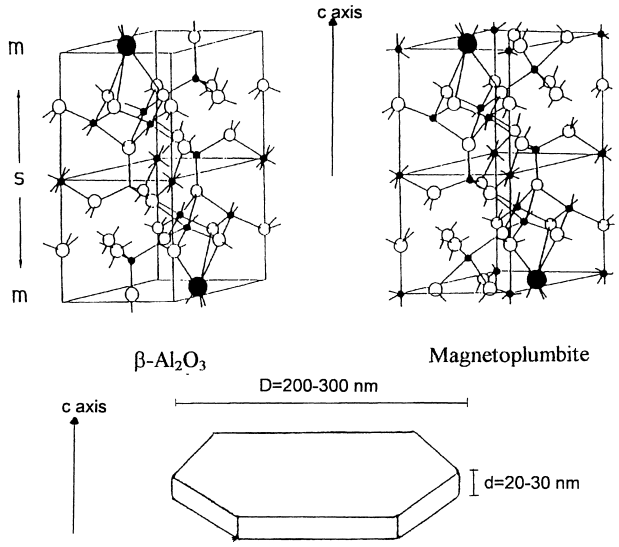

Fig. 12. Crystal structure of β-Al_2O_3 and magnetoplumbite phases. (●), Alkali, alkali-earth or rare-earth ions; (○), oxygen ions; and (●), aluminium ions.

These materials, containing transition metal ions in the structure, were prepared by hydrolysis of the alkoxides [23,60–62] or by co-precipitation from the nitrates of the constituents by using $(NH_4)_2CO_3$ as a precipitating agent [63–66]. Monophasic samples with a layered alumina structure and surface areas in the range of 10–15 m^2/g were obtained upon calcination at 1300°C. The sintering resistance of hexaaluminates is strictly related to their layered structure [58] that can be classified into two types: magnetoplumbite and β-Al_2O_3. As shown in Fig. 12, they both consist of closely packed spinel blocks separated by mirror planes that contain large cations of alkali, alkali-earth and rare-earth ions and loosely packed oxygen ions. Spinel blocks and mirror planes are alternatively stacked, originating a hexagonal structure with the *c*-axis parallel to the direction of stacking. The two structures differ in the composition of the mirror plane. These materials crystallise as hexagonal planar particles with marked anisotropic shape because the crystal growth along the *c*-axis is suppressed due to inhibition of ions diffusion along the stacking direction.

In view of close similarity of ionic radii, transition metal ions (M = Mn, Cu, Fe, Cr, Co, Ni) can partially substitute Al ions. The transition metal ions provide significant activity in combustion, since this reaction occurs via a redox mechanism with variation of the oxidation state of the metal. A volcano-type correlation has been observed between catalytic activity and difference of standard formation enthalpies of trivalent and divalent metal-oxides, where Mn is the most active element. Mn was demonstrated to enter the structure at low concentrations ($x \leq 1$ in $BaMn_xAl_{12-x}O_{19}$), preferentially in tetrahedral Al(2) sites with dominant oxidation state 2+, with concomitant reduction of the Ba vacancies in the mirror plane due to a charge compensation mechanism, and at high concentrations ($2 \leq x \leq 3$ in $BaMn_xAl_{12-x}O_{19}$) in octahedral Al(1) sites with the dominant oxidation state 3+ [67]. Introduction of even higher Mn amount results in the segregation of extra phases ($BaAl_2O_4$) and in a marked drop of surface area.

The catalytic activity of substituted hexaaluminates has been investigated in the literature mainly over powder catalysts in a lab scale micro-reactor [60–66]. Methane conversion curves are reported in Fig. 13 for $BaMn_xAl_{12-x}O_{19}$ catalysts with different Mn content. The catalytic activity increases with Mn loading up to $x = 2$, keeps constant for $x = 3$ and then decreases: the temperature at which 20% conversion is obtained shifts from 660°C for $x = 0.5$ to 560°C for $x = 2$ and $x = 3$, and then back to 700°C for $x = 4$. The conversion

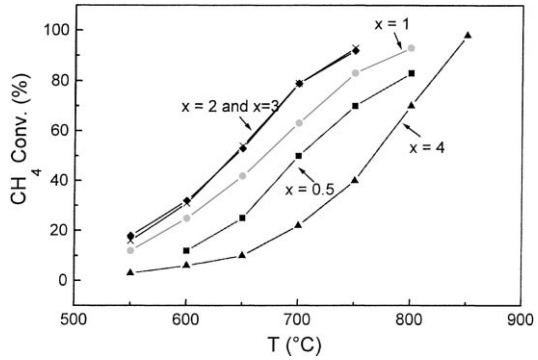

Fig. 13. CH_4 combustion activity of BaMnxAl12-*x*O19 [59]. Results of tests over catalyst powders at GHSV=48000 h^{-1} with CH_4 (1% v/v) in air.

curves for CO and H_2 combustion [68,69] confirmed a much higher reactivity of Mn-substituted hexaaluminates towards these fuels: 20% conversion were measured over $BaMnAl_{11}O_{19}$ at $T = 260°C$ for CO and $T = 370°C$ for H_2, by operating with the same fuel concentration and GHSV of Fig. 13. The catalytic activity is also influenced by the composition in the mirror plane: maximum catalytic activity is reported by Arai et al. [70] for $Sr_{0.8}La_{0.2}MnAl_{11}O_{19}$. This activity, however, is comparable to that of $BaMn_2Al_{10}O_{19}$.

Mathematical models of monolithic combustor were used for extrapolation of the laboratory-scale data to industrial operating conditions in the case of $BaMn_2Al_{10}O_{19}$. [71]. Simulation results pointed out that in CH_4combustion ignition occurs only above 750–800°C. Accordingly, hexaaluminates can be used as end-stage catalysts in segmented configurations to provide high gas temperature at the exit of the catalyst section. This is in line with the configuration adopted by Osaka Gas [12]. In the case of CO/H_2 containing mixtures, the ignition temperature over hexaaluminates is ca. 300°C lower than with CH_4, but it is still not low enough to fulfill the requirements of gas turbine combustor in most demanding conditions (idle and partial load).

4. Catalytic combustion of fuels other than natural gas

There is a growing interest in the use of low-heating-value (LHV) fuels obtained by gasification of coal, tars, biomass and wastes as alternative fuels or diesel oils (primarily) as back-up fuels in catalytic combustion for GT application.

The authors are being involved in an EU programme aimed at the development of an *U*ltra-*L*ow-*E*mission-*CAT*alytic combustor (ULECAT) for GT, able to run with both gasified biomasses and diesel fuels. Catalyst development and testing is the main target of the project. The following conclusions have been drawn so far from the study [72–74]:

1. Scale-up of the activity data collected at the lab-scale by means of mathematical modelling showed that Mn-substituted hexaaluminates are not active enough to satisfy the operating requirements of catalytic combustors fuelled by gasified biomasses. This is due to the relatively high methane content of the fuel that requires noble metals based-catalysts for ignition at low temperature.
2. High catalytic activity has been measured for palladium based catalysts developed by IFP in both, the combustion of gasified biomasses and synthetic diesel fuel.
3. Both, palladium-based and Mn-substituted hexaaluminate catalysts are very active in the oxidation of ammonia to NO. However, at high temperatures a decrease in the NO formation is observed, paralleled by the production of N_2, possibly through selective non-catalytic reduction (SNCR) mechanism. This aspect deserves further investigation, being relevant to the reduction of undesired fuel-NO_x.
4. Over Pd catalysts, combustion of CO and H_2 is not affected by sulphur compounds, whereas methane combustion is markedly depressed. Over Mn-substituted hexaaluminates, a severe deactivation was observed for all fuel components (CO, H_2, CH_4, C_2H_4) and Ba-containing materials were irreversibly poisoned.
5. Preliminary results, collected at the pilot scale under atmospheric pressure, documented light-off performances in line with the predictions set forth on the basis of laboratory tests and by using mathematical modelling.
6. For combustion of diesel fuel, problems associated with slow rate of gas-solid diffusion and high homogeneous reactivity should be carefully addressed for the different system configurations.

Further work must be performed at conditions of real interest for industrial applications to assess the feasibility of the dual fuel catalytic combustor.

5. Mathematical models of catalytic combustors

Mathematical models represent a powerful tool for the design, analysis and operation of catalytic combustor for gas turbines. In the following, the major features of mathematical models of the catalyst and homogeneous sections, that have been extensively reviewed in [11,75], are briefly addressed.

5.1. Modelling of the catalyst section

Single channel models are customarily used since assuming global adiabaticity and uniform distribution of the variables at the catalyst inlet section, all the channels operate under identical conditions. Both these multi-dimensional models, accounting for the variable distribution over the channel cross section and periphery (distributed models), and 1-D models, based on lumping of the cross section and peripheral distributed variables into appropriate average values (lumped models), of the monolith single channel have been developed in the literature.

In principle, many phenomena have to be included in the model:

1. heterogeneous reactions at the catalyst wall and homogeneous reactions in the gas phase;
2. heat, mass and momentum transfer by convection and diffusion in the gas phase and at the gas-solid interface, that are markedly affected by entrance effects;
3. mass and heat diffusion in the active catalyst phase; and
4. peripheral and axial heat transfer in the solid phase through active washcoat and substrate by conduction and radiation.

In view of the number of complex phenomena to be accounted for and considering strong non-linearity associated with temperature effects, the computational labour for solution of the governing equations of rigorous models is tedious so as to make any adequate approximation quite attractive.

The following aspects on the relative importance of the above phenomena have been assessed by comparing simulation results of progressively simplified models with those of a rigorous one under laminar flow conditions [71,76–78]. Such conditions correspond to the lowest limit of operation of hybrid catalytic combustors and to standard conditions of pilot catalytic combustor operated at atmospheric pressure.

1. Inlet effects associated with the development of temperature and concentration profiles must be accounted for due to the short axial length of the catalyst segments.
2. The temperature dependence of the gas properties must be included since it markedly affects the performances of the combustor.
3. The contribution of axial heat conduction in ceramic monoliths can be neglected as compared to the extremely high convective transport.
4. For similar reasons and also in view of typical high aspect ratios, the contribution of heat radiation can be neglected, but for heat dispersion effects at the catalyst ends [79].
5. Intra-phase diffusion has to be accounted for since it does affect the ignition behaviour. E.g. diffusion barriers are used to control catalyst temperature runaway in methane combustion [49].
6. The relevance of homogeneous reaction within the catalyst section depends markedly on the type of fuel, and appears to be negligible for methane. However in order to quantify more precisely its contribution detailed kinetic schemes have to be considered.
7. Lumped models, incorporating correlations for local heat and mass gas-solid transfer coefficients that take into appropriate account boundary conditions and channel geometry, can be adequate but for the accurate prediction of the light-off behaviour.

Under turbulent or transitional-flow conditions, that prevail under most operation regimes of GT combustors, modelling of monolithic channels suffers from the great complexity of the hydrodynamic phenomena. In particular, for a transitional regime neither accurate correlations for heat/mass transfer coefficients in 1-D models, nor rigorous distributed descriptions are available.

In addition to theoretical investigations on the relative importance of the several physico-chemical phenomena that might affect the combustor performances, some practical applications of mathematical models of

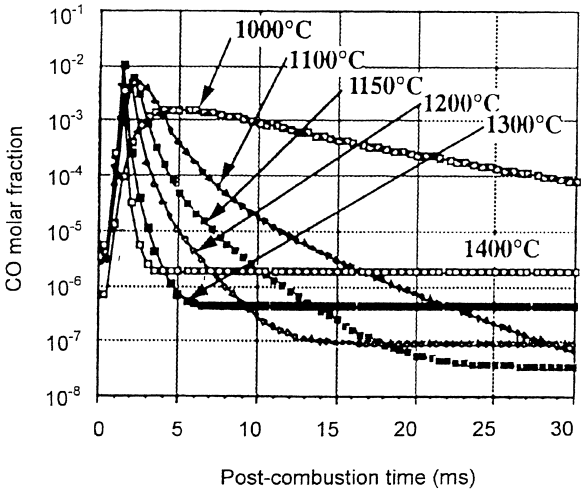

Fig. 14. Calculated profiles of CO concentrations in the afterburner section of a partial combustor [82].

the catalyst section are documented in the literature. Examples are: prediction of the activity levels required to achieve ignition at relevant operating conditions and scale up of laboratory-scale data [56,71]; evaluation of thermal stresses of the catalyst [80]; determination of the thickness of an inert diffusional barrier required to effectively reduce the reaction rate at the catalyst inlet, thus mitigating runaway phenomena [81]. Nevertheless, the use of mathematical models for practical purposes is still limited and strong validation efforts are required to establish simulation codes as current design tools.

5.2. Modelling of the homogeneous section

The use of consolidated detailed kinetics for gas phase combustion can provide guide-lines for operation in the homogeneous section in order to match emission targets within reasonable constraints on combustor size.

Dalla Betta and Loffler [82] simulated the homogeneous radical reaction downstream of the catalyst section using a simplified version of the kinetic model of Miller and Bowman and assuming a plug flow reactor model. Simulation results reported in Fig. 14 show that CO is an intermediate product and that, for a constant catalyst exit temperature of 950°C, the CO concentration strongly depends on the combustor-outlet temperature and the residence time. Considering that the target CO emission is 10 ppm and the residence time in a typical GT combustor is of 10–30 ms, the combustor outlet temperature should be 1100°C or higher (and the catalyst exit temperature sufficiently high).

6. Future research opportunities

Areas where future research activities could be recommended are specified below:

1. Additional tests at the pilot and full-scale laboratory and field level have to be done to improve the reliability of the most promising system configurations and to address the issues still open These include long-term performances of the catalyst and of the different components of the combustor, enlargement of the load range of operation, improvement of coupling between the heterogeneous and the homogeneous sections, establishment and validation of the control method, specifications for natural gas and other fuels.
2. The use of fuels other than methane as alternative fuels and/or back-up fuels has to be investigated more extensively. In the case of LHV fuels the identification of the optimal thermodynamic cycle and the definition of the combustor lay out may also be considered.
3. The dynamics of the PdO–Pd transformation at the temperature levels of interest for industrial applications, which is of relevance for ignition runaway, has to be studied more in details and compared to the dynamics of the combustion reactions. Besides, several other features of Pd catalysts, are not yet fully understood, deserve additional fundamental investigations.
4. There is still a need for catalyst with enhanced activity to light off the fuel mixture at the temperature of air delivered from the compressor. Any improvement in the basic understanding of active Pd catalysts may provide a chance in this respect.
5. More reliable and comprehensive chemical kinetic rate expressions based on experimental data collected under conditions as close as possible to those of industrial interest are required for a proper design of catalytic combustors. A contribution along these lines may be provided by the development and use of experimental devices

specifically designed for this purpose, such as the annular reactor mentioned in the text.

6. More sophisticated modelling of the catalyst section, and of the homogeneous section, can be attempted to provide an improved description of the several complex phenomena that govern the process. In any case, model validation by comparison of model predictions and experimental results is rather scarce so far. This is mainly due to the lack of detailed experimental data at full scale and to the fact that experimental and modelling works are carried out by different research groups. Joint efforts from experimental and theoretical research groups are strongly recommended.

Other aspects that have not been addressed in this paper need further study. These include investigation on structural and catalytic durability of combustion catalysts at high temperatures and also development of improved pre-burned designs with lower formation of NO_x.

Acknowledgements

The authors acknowledge the financial support of MURST (Rome, Italy). Thanks are also due to Drs. Dalla Betta and McCarty of Catalytica Inc. and to Dr. Sadamori of Osaka Gas for providing valuable unpublished material.

References

[1] D.L. Trimm, Appl. Catal. 7 (1983) 249.
[2] R. Prasad, L.A. Kennedy, R.E. Ruckenstein, Catal. Rev. Sci. Eng. 26 (1984) 1.
[3] J.P. Kesserling, in: F.J. Winberg (Ed.), Advanced Combustion Methods, Academic Press, London, 1986.
[4] L.D. Pefferle, W.C. Pfefferle, Catal. Rev. Sci. Eng. 29 (1987) 219.
[5] M. Zwinkels, S. Jaras, P.G. Menon, Catal. Rev. Sci. Eng. 35 (1993) 319.
[6] S.T. Kolaczkowski, Trans. I. Chem. Epart A 73 (1995) 168.
[7] K. Eguchi, H. Arai, Catal. Today 29 (1996) 379.
[8] R.A. Dalla Betta, Catal. Today 35 (1997) 129.
[9] J.G. McCarty, M. Gusman, D.M. Lowe, D.L. Hildenbrand, K.N. Lau, Catal. Today 47 (1999) 5.
[10] J.G. McCarty. 3rd Europacat, Krackow, September 1997, Plenary lecture.
[11] G. Groppi, E. Tronconi, P. Forzatti, Catal. Rev. Sci. Eng. 41(2) (1999) 227.
[12] H. Sadamori, Catal. Today 47 (1999) 325.
[13] J. Saint-Just, J. Der Kinderen, Catal. Today 29 (1996) 387.
[14] S. Ro, A. Scholten, Catal. Today 47 (1999) 415.
[15] Buderus Heiztechnik, EP Appl. 93110601.9 (12.1.94).
[16] G. Saracco, I. Cerri, V. Specchia, R. Accornero, Proceedings of ISCRE15, Newport Beach, 13–16 September 1998, p. 290.
[17] Z.R. Ismagilov, M.A. Kenzhentsev, Catal. Rev. Sci. Eng. 31 (1990) 51.
[18] I. Stambler, Gas Turbine World, March (1993) p. 23.
[19] H. Sadamori, T. Tanioka, T. Matsuhisa, Catal. Today 26 (1995) 337.
[20] M. Machida, K. Eguchi, H. Arai, Chem. Letts. (1987) p 767.
[21] Y. Ozawa, Y. Tochihara, N. Mori, I. Yuri, T. Kanazawa, K. Sagimori, ASME Paper 98-GT-381, 1998.
[22] R.A. Dalla Betta, N. Ezawa, K. Tsurumi, J.C. Schlatter, S.G. Nickolas, US Patent 5183401, 2 February 1993.
[23] R.A. Dalla Betta, K. Tsurumi, N. Ezawa, US Patent 5232257, 3 August 1993.
[24] R.A. Dalla Betta, F.H. Ribeiro, T. Shoji, K. Tsurumi, N. Ezawa, S.G. Nickolas, US Patent 5250489, 5 October 1993.
[25] J.C. Schlatter, R.A. Dalla Betta, S.G. Nicholas, M. B. Cutrone, K.W. Beebe, T. Tsuchiya, ASME Paper 97-GT-57, 1997.
[26] R.A. Dalla Betta, J.C. Schlatter, S.G. Nicholas, M.B. Cutrone, K.W. Beebe, Y. Furuse, T. Tsuchiya, ASME Paper 96-GT-485, 1996.
[27] R.J. Farrauto, M.C. Hobson, T. Kennelly, E.M. Waterman, Appl. Catal. A: Gen. 81 (1992) 227.
[28] Unpublished results from our laboratory.
[29] J. Chen, E. Ruckenstein, J. Catal. 69 (1981) 254.
[30] J. Chen, E. Ruckenstein, J. Phys. Chem. 85 (1981) 1606.
[31] E. Ruckenstein, J. Chen, J. Catal. 70 (1981) 233.
[32] E. Ruckenstein, J. Chen, J. Coll. Interface Sci. 86 (1982) 1.
[33] H. Lieske, J. Volter, J. Phys. Chem. 89 (1985) 1841.
[34] R.F. Hicks, H. Qi, M.L. Young, R.G. Lee, J. Catal. 122 (1990) 295.
[35] E. Garbowski, C. Feumi-Jantou, N. Mouaddid, M. Primet, Appl. Catal. A: Gen. 109 (1994) 277.
[36] R. Burch, F.J. Urbano, Appl. Catal. A: Gen. 124 (1995) 121.
[37] K. Otto, C. Hubbard, W. Weber, G. Graham, Appl. Catal. B: Environm. 1 (1992) 317.
[38] A. Ogata, A. Obuchi, K. Mizuno, A. Ohi, H. Obuchi, J. Catal. 144 (1993) 452.
[39] J.W.M. Jacobs, D. Schryvers, J. Catal. 103 (1987) 436.
[40] T. Fleish, R. Kicks, A. Bell, J. Catal. 87 (1984) 398.
[41] S.C. Su, J.N. Carstens, A.T. Bell, J. Catal. 176 (1998) 125.
[42] E. Voogt, PhD Thesis, University of Utrecht, 1997.
[43] J. McCarty, Catal. Today 26 (1995) 283.
[44] M Lyubovski, R. Weber, L. Pfefferle, 26th International Symposium on Combustion, 1779, 1996.
[45] J.N. Carstens, S.C. Su, A.T. Bell, J. Catal. 176 (1998) 136.
[46] M. Lyubovsky, L. Pfefferle, Appl. Catal. A: Gen. 173 (1998) 107.
[47] K. Fujimoto, F.H. Ribeiro, M. Avalos-Borja, E. Iglesia, J. Catal. 179 (1998) 431.
[48] T. Griffin, W. Weisenstein, V. Scherer, M. Fowles, Combust. Flames 101 (1995) 81.
[49] R.A. Dalla Betta, K. Tsurumi, T. Shoji, R.L. Garten, US Patent 5405260, 11 April 1995.

[50] Y.Y. Yao, Ind. Eng. Chem Prod. Res. Dev. 19 (1980) 293.
[51] S.H. Oh, P.J. Mitchell, R.M. Siewert, J. Catal. 132 (1991) 287.
[52] P. Briot, M. Primet, Appl. Catal. 68 (1991) 301.
[53] T.R. Baldwin, R. Burch, Appl. Catal. 66 (1990) 337.
[54] F.H. Ribeiro, M. Chow, R.A. Dalla Betta, J. Catal. 146 (1994) 537.
[55] J.C. van Giezen, PhD Thesis, the University of Utrecht, 1997.
[56] R.A. Dalla Betta, J.C. Schlatter, D.Y. Kee, D.G. Loffler, T. Shoji, Catal. Today 26 (1995) 329.
[57] A. Beretta, P. Baiardi, D. Prina, P. Forzatti, Chem. Eng. Sci. 54 (1999) 765.
[58] H. Arai, US Patent 4788174, 29 November 1988.
[59] G. Groppi, C. Cristiani, P. Forzatti, Catal. 13 (1997) 85.
[60] M. Machida, K. Eguchi, H. Arai, J. Catal. 103 (1987) 385.
[61] M. Machida, K. Eguchi, H. Arai, Bull. Chem. Soc. Jpn. 61 (1988) 3659.
[62] M. Machida, K. Eguchi, H. Arai, J. Catal. 120 (1989) 377.
[63] G. Groppi, M. Bellotto, C. Cristiani, P. Forzatti, P.L. Villa, Appl. Catal. A 104 (1993) 101.
[64] G. Groppi, M. Bellotto, C. Cristiani, P. Forzatti, J. Mat. Sci. 29 (1994) 3441.
[65] G. Groppi, F. Assandri, M. Bellotto, C. Cristiani, P. Forzatti, J. Sol. Stat. Chem. 114 (1995) 326.
[66] G. Groppi, C. Cristiani, P. Forzatti, J. Catal. 168 (1997) 95.
[67] M. Bellotto, G. Artioli, C. Cristiani, P. Forzatti, G. Groppi, J. Catal. 179 (1998) 597.
[68] G. Groppi, A. Belloli, E. Tronconi, P. Forzatti, Catal. Today 29 (1996) 403.
[69] C. Cristiani, G. Groppi, P. Forzatti, E. Tronconi, G. Busca, M. Daturi, Studies Surf. Sci. Catal. 101 (1996) 473.
[70] M. Machida, K. Eguchi, H. Arai, J. Catal. 123 (1990) 477.
[71] G. Groppi, E. Tronconi, P. Forzatti, Appl. Catal. A 138 (1996) 177.
[72] G. Groppi, L. Lietti, E. Tronconi, P. Forzatti, Catal. Today 45 (1998) 159.
[73] M. Johansson, PhD Thesis, KTH, Sweden, 1998.
[74] J.H. Legal, G. Martin, D. Durand, ASME paper 98-GT-294, 1998.
[75] R.E. Hayes, S.T. Kolackzowski, Introduction to Catalytic Combustion, Gordon and Breach, 1997.
[76] G. Groppi, A. Belloli, E. Tronconi, P. Forzatti, A.I.Ch.E. J. 41 (1995) 2250.
[77] G. Groppi, A. Belloli, E. Tronconi, P. Forzatti, Chem. Eng. Sci. 50 (1995) 2705.
[78] E. Tronconi, P. Forzatti, A.I.Ch.E. J. 38 (1992) 201.
[79] R.E. Hayes, S.T. Kolackzowski, W.J. Thomas, Comp. Chem. Eng. 16 (1992) 645.
[80] Y. Tsujikawa, S. Fujii, H. Sadamori, S. Ito, S Katsura, ASME Paper, 95-GT-351, 1995.
[81] D. Leung, R.E. Hayes, S.T. Kolackzowski, Can. J. Chem. Eng. 74 (1996) 94.
[82] R.A. Dalla Betta, D.G. Loffler, ACS Symp. Ser. Heterogeneous Hydrocarbon Oxidation, 638 (1996) 36
[83] H. Kleykamp, Z. Physik. Chem. N.F. 71 (1970) 142.